Chapter 11
Manufacturing and Evaluation of Corrosion Resistance of Nickel-Added Co–30Cr–4Mo Metal Alloy for Orthopaedic Biomaterials

Amit Aherwar

1 Introduction

Today, the major problem faced by a doctor and researcher in the field of orthopaedic materials is the selection of right biomaterials with correct proportions. Metallic materials such as stainless steel (SS), cobalt–chromium alloys (Co–Cr) and titanium and titanium alloys (Ti) are the effective orthopaedic materials used for implants. Table 1 lists the various materials including metallic, composites, ceramic and so on are used in orthopaedic application [1–3], and Table 2 lists the various possible material combinations of orthopaedic implants [4, 5]. These combinations of metallic biomaterials as listed in Table 2 have good corrosion resistance, good mechanical properties and biocompatibility, which make them a splendid choice for orthopaedic applications [6]. However, instead of these properties, there is some flaw in the metallic orthopaedic materials such as high elastic modulus, which causes stress shielding and corrosive nature. Corrosion deteriorates the implant materials in the form of metal ions and these ions liberated into the tissue resulting in adverse reactions [7]. 316 and 316L grades of stainless steel are the prime grades utilized to manufacture artificial bone as it is easy to cast into distinct shapes and sizes. Grade 316L has a healthier corrosion resistance as compared to 316 grades due to the attendance of less percentage of carbon content in the matrix alloy. Both 316 and 316L grades of stainless steel are easy to make fracture plates, screws, and hip nails. Due to ease of fabrication and desirable assortment of mechanical properties, corrosion behaviour, stainless steel becomes the predominant implant alloy [8]. Based on the superior results, ASTM has strongly recommended 316L grade as a foremost alloy for implant production [9, 10]. However, one more metallic material such as cobalt-based alloys are amid the most favourable orthopaedic biomaterials for making implants components such as

A. Aherwar (✉)
Mechanical Engineering Department, Madhav Institute of Technology and Science, Gwalior 474005, India
e-mail: amit.aherwar05@gmail.com; amit.aherwar05@mitsgwalior.in

Table 1 Various materials used in orthopaedic application

Materials		Applications	References
Metals	SS-316L	Used in femoral head and stem components	[7, 8, 12]
	Co alloys	Used in femoral heads and stems, porous coatings, tibial and femoral components	
	Cast CoCrMo Wrought Co–Ni–Cr–Mo Wrought Co–Cr–W–Ni		
Titanium-based materials	CP Ti	Used in porous coatings second phase in ceramic and PMMA composites	[10]
	Ti_6Al_4V	Used in femoral heads and stems, porous coatings, tibial and femoral components	
	$Ti_5Al_{2.5}Fe$	Used in femoral head and stem components	
	Ti–Al–Nb	Used in femoral head and stem components	
Ceramics	Bioinert		[24–26]
	Carbon	Used in metal coatings on femoral stem components, second phase in composites and bone cement	
	Alumina	Used in femoral stems heads and acetabular cup components	
	Zirconia	Used in femoral stems and acetabular cup components	
Polymers	PMMA	Used in acetabular cups, tibial and patellar components	[27]
	UHMWPE/HDPE	Used in porous coatings on metallic and ceramic femoral stem components	
	Polysuffolene	Used in femoral stems, porous coatings on metallic femoral stem components	
	PTFE	Used in femoral stems, porous coatings on metallic femoral stem components	

Table 2 Materials' combination used in orthopaedic hip implants

Material used for Femoral-Socket component	Results	References
CoCrMo–CoCrMo	Aseptic loosening rate is high, restricted use, minimum wear rate	[19, 21–23]
CoCrMo-UHMWPE	Widely in use, minimum wear loss	[21–23]
Alumina/zirconia-UHMWPE	Minimum wear rate	[10, 24–26]
Alumina–Alumina	Low wear rate, problem of joints pain	[10, 24]
Ti_6Al_4V-UHMWPE	Maximum wear	[27]
Surface-coated Ti_6Al_4V-UHMWPE	Better wear resistance to abrasion, attained skinny layer	[27]

hip and knee joints, owing to their excellent mechanical strength and corrosion resistance [11]. Co–Cr alloy is commonly utilized as implants and fixations due to much attuned with the human body. In contrast with further biomaterials, Co–Cr alloys have a good biocompatibility property than SS (Both 316 and 316L) alloys but lesser than titanium alloys. Basically, Co-based alloys can be cast, wrought, or forged [12]. Accumulation of nickel in the modified $Co_{30}Cr_4Mo$ alloy enhances the corrosion properties due to slow rate oxidation and improved the mechanical properties [13, 14]. The density of pure nickel is 8.89 g/cm^3; melting temperature is 1468 °C and an elastic modulus of 209 GPa. Nickel specifically stabilizes the FCC structure and gives strength of the modified alloy. In fact, Nickel also improves the workability and castability of the alloy [15]. This element is considered corrosion-resistant due to its slow rate of oxidation in air at room temperature. Nevertheless, when metal alloys are used as implants and subjected to the body fluid, corrosion is inevitable. Corrosion is a continual process taking place on the surface of metals releasing ions into the surrounding media [16–20]. These ions may be biologically active and potentially carcinogenic [21, 22]. Therefore, all-inclusive knowledge of the effect of these ions on the surrounding tissues is requisite and attempts should be made to prevent the associated adverse effects. For example, the oxidation of Co–Cr–Mo routinely produces Co and Cr cations found in serum of patients with prosthesis, and molybdenum forms ionic species soluble in water; which are toxic [23, 24]. Depending on the nature and concentration of such chemical species, numerous inimical reactions may take place including allergy, infections, metallosis, skin toxicity, and many more [25, 26]. Therefore, Co–Cr–Mo alloy still lacks enough corrosion resistance to perform successfully in long-term use in the human body. This is of critical importance for implants with metal-on-metal (MoM) components such as MoM hip prostheses [27].

The authors in their earlier work [9] manufactured Co–30Cr alloys with modified molybdenum (Mo) content as potential biomaterials for hip implants and optimize it. Furthermore, analysis of variance (ANOVA) was also implemented to investigate the effect of molybdenum on mechanical and wear properties. From their results, it was concluded that the 4 wt% molybdenum alloying element provides minimal material loss. In the continuation of previous study, therefore, the present study manufactures

the orthopaedic material consisting of $Co_{30}Cr_4Mo$ alloy as a base matrix and nickel as a filler to improve the properties of designed biomaterials and assess their properties with the focus on corrosion behaviour which has still remained as one of the most challenging clinical problems.

2 Test Materials and Methods

2.1 Test Materials

Mittal Industries, India, supplied the grades of raw materials such as Cobalt (Co), Chromium (Cr), Molybdenum (Mo) and Nickel (Ni) to make test specimens with distinct wt% Ni, in which cobalt was in ingot form and the rest were in powders form with size of below 44 μm. The micrographs of all the alloying elements are shown in Fig. 1. Furthermore, the element content with weight percentage of the manufactured alloys is listed in Table 3.
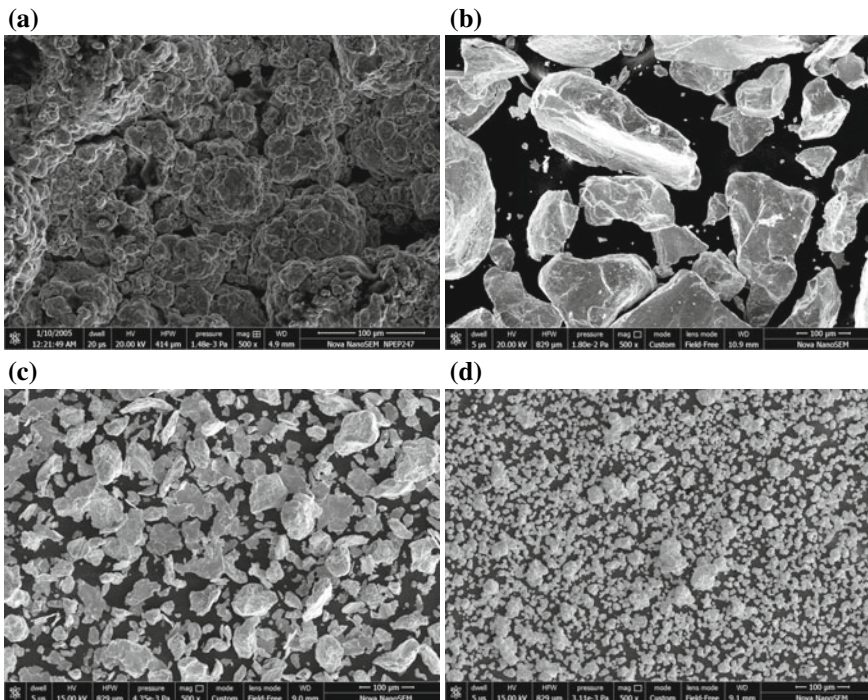
(a)   **(b)**

(c)   **(d)**

Fig. 1 FESEM micrograph of **a** cobalt, **b** chromium, **c** molybdenum, **d** nickel

Table 3 Element content and designation of specimens (in weight percentage)

Sample designation	Elements			
	Co	Cr (%)	Mo (%)	Ni (%)
N0	Bal	30	4	0
N1	Bal	30	4	1
N2	Bal	30	4	2
N3	Bal	30	4	3
N4	Bal	30	4	4

2.2 Manufacturing of Orthopaedic Material

The schematic view of vacuum-based casting set-up used for manufacturing orthopaedic materials is shown in Fig. 2. In the presented work, five plates (100 mm × 65 mm × 10 mm) with x wt% of Ni ($x = 0, 1, 2, 3$ and 4) added Co–30Cr–4Mo alloy were produced using an induction furnace according to the composition. In this apparatus, there are two separate sections available in the set-up: (1) melting section and (2) casting section. A chiller unit is also attached in the set-up. Here, both the sections are under vacuum background. A motor was coupled with the bottom section and set to be around 200 rpm for proper mixing of all the metals present in the matrix. For manufacturing, all the proposed materials with respective weight percentages were melted above 1800 °C for 12 min and then dropped downwards into the graphite mould (100 mm × 65 mm × 10 mm) with the help of plunger under vacuum conditions. After casting, the mould was removed and then cut as per the sample size.
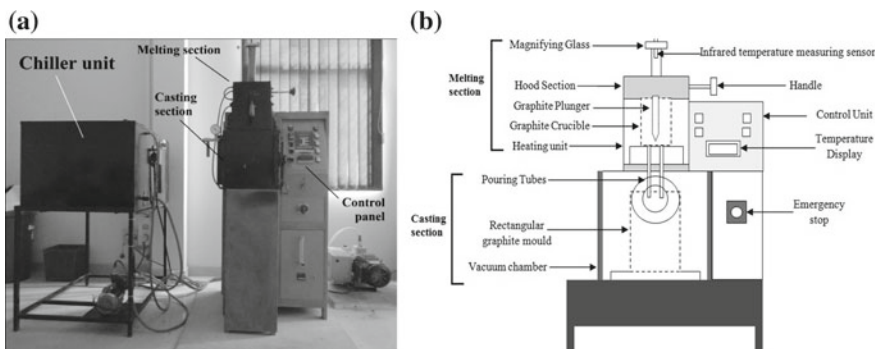

Fig. 2 Experimental set-up of casting machine, **a** image of the casting set-up, **b** schematic diagram of the casting machine used for making the specimens

2.3 Material Characterization

The morphology of materials was characterized using FESEM and EDS of FEI Nova Nano SEM 450. The phase and crystal structure of the manufactured orthopaedic materials were studied using XRD and for the same PANalytical X'Pert PRO X-Ray diffractometer was utilized. The fabricated samples were polished by using Buehler MetaServ 250 polisher/grinder. After polishing, the specimens were etched for 12 s.

2.4 Mechanical Studies

Micro-hardness evaluation was carried out by USL micro-hardness tester. A diamond indenter was forced into the manufactured specimen under a load of 0.5 N for 10 s. The density of the manufactured alloys was recorded by the Archimedian principle. For measurement of physical and mechanical properties, three specimens were tested and the mean value was recorded for more precise results.

2.5 Electrochemical Test

The electrochemical behaviour and corrosion resistance of the manufactured alloys were investigated in the most unfavourable environment with aggressive pH (NaCl solution). It is unfeasible to accomplish corrosion tests on these orthopaedic biomaterials by the weight loss methodology since their rate of corrosion is acutely small and it takes a lengthy to obtain results. Thus, the foremost widespread method in corrosion studies, which is the recording of anodic polarization curves by the employment of the Tafel method, was used in this study. Electrochemical tests were conducted in a corrosion cell (see Fig. 3) using three electrodes; one was working electrode whose degradation property has to be tested, the second electrode was graphite as the auxiliary/counter electrodes and the third electrode used was saturated calomel electrode (SCE) which was used to sense the reaction happening within the corrosion cell and to input the values to the software where necessary data was shown in the form of graphs. GAMRY potentiostat VFP600 instrument was employed for performing electrochemical tests by accelerating corrosion with appropriate current and voltages. This instrument was allied to a PC and accessed with the assistance of Gamry Framework software. A potentiostat with corrosion software (Echem Analyst) was utilized for data analysis. The corrosion current density (i_{corr}) and other corrosion parameters were calculated from the polarization curves by Tafel extrapolation. Saline solution was prepared using 8 g/L NaCl, with pH 7.4 at the body temperature (37 °C). The capacity of the cell was 100 ml. The anodic polarization curve for the Tafel analysis was measured from -150 to $+150$ mV v/s E_{corr} with a scanning rate of 1 mV/s after immersing in electrolyte about 30 min. The potentiodynamic curves
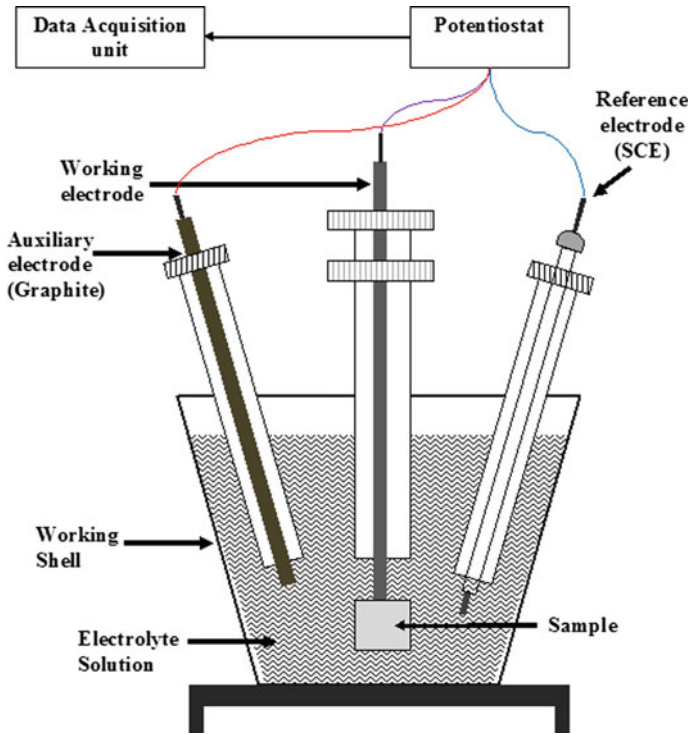
Fig. 3 Electrochemical test set-up

were recorded at a constant voltage scan rate of 10 mV/s. The specimen area exposed was 8 cm^2 with scan frequencies ranging from -1 to 1 V.

In order to compute the i_{corr}, usually, the Stern-Geary equation is used as shown in Eq. (1). Since it was not possible to evaluate the coefficient value of Tafel's b_a and b_c, corrosion current was estimation using approximated Stern-Geary's Eq. (2).

$$i_{corr} = \frac{b_a \times b_c}{2.3(b_a + b_c)R_p} \tag{1}$$

$$i_{corr} = \frac{0.026}{R_p} \tag{2}$$

where b_a is a slope coefficient of the anodic Tafel line; b_c is a slope coefficient of the cathodic Tafel line and R_p is a polarisation resistance (Ωcm^2).

Meanwhile, the surface micrographs of all samples after immersion in saline (NaCl) solution at 37 °C with pH of 7.4 were provided for further evaluation.

3 Results and Discussion

3.1 Micro-structure and Phase Analysis of Materials

The XRD patterns of all the alloys are presented in Fig. 4. The micro-structure of nickel-free alloy showed a cobalt matrix with chromium and molybdenum regions. The HCP structure of Co has been formed due to martensitic transformation [28, 29]. None of carbide particles are shown in the micro-structure, which corresponds healthy with the XRD peaks observed in 0–4 wt% Ni. Moreover, the compounds cobalt (Co), chromium (Cr), molybdenum (Mo) and nickel (Ni) can be seen clearly confirming its presence (Fig. 4) in the matrix. The lattice parameters which were detected are provided in Table 4. The peaks recorded in this study are alike from the previous studies [30–32]. Scanning electron micrographs and their corresponding EDX results are shown in Fig. 5.

3.2 Mechanical Studies of Manufactured Material

The test results of the physical and mechanical strength of the manufactured alloys with different nickel concentration (Co–30Cr–4Mo) are listed in Table 5. The obtained results show that the density significantly increased with the
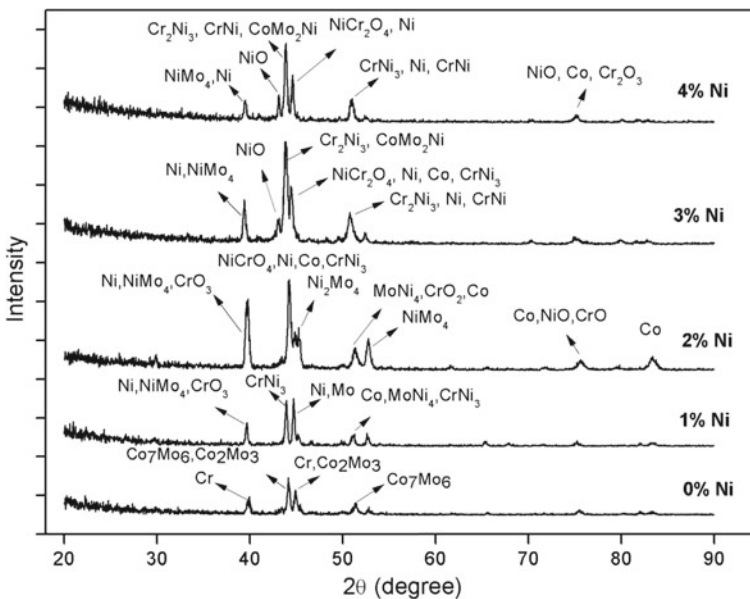

Fig. 4 XRD of the $Co_{30}Cr_4Mo$ alloy with 0–4 wt% of nickel content

Table 4 Identified phases and the lattice parameters

Phases	Crystal structure	Lattice parameters
Cobalt base α matrix	FCC (111)	$d = 2.04$ Å, $a = b = c = 3.545$ Å
Cr	BCC (110)	$d = 2.039$ Å, $a = b = c = 2.884$ Å
Mo	BCC (110)	$d = 2.225$ Å, $a = b = c = 3.147$ Å
$CrNi_3$	Cubic (111)	$d = 2.0507$ Å, $a = b = c = 3.552$ Å
Co_2Mo_3	Tetragonal (411)	$d = 2.0311$ Å, $a = b = 9.229$ Å and $c = 4.827$ Å
Co_7Mo_6	Rhombohedral (116)	$d = 2.08$ Å
Co_7Mo_6	Rhombohedral (027)	$d = 1.796$ Å $a = b = 4.762$ Å, and $c = 25.617$ Å
$MoNi_4$	Tetragonal (002)	$d = 1.782°$A, $a = b = 5.724$ Å, $c = 3.564$ Å
$NiCr_2O_4$	Cubic (220)	$d = 2.9407$ Å, $a = b = c = 8.318$ Å
$NiCrO_3$	Rhombohedral (104)	$d = 2.648$ Å, $a = b = 4.925$, $c = 13.504$ Å

incorporation of nickel concentration. The densities obtained from the test results are close to ASTM F75 [33].

3.3   Micro-hardness

The Vickers micro-hardness characteristics were measured at six distinct spots and the average value was taken. Table 5 represents the values of micro-hardness of the manufactured alloys. It was observed that the hardness of the nickel-added Co–30Cr–4Mo alloy increases linearly with the increase in nickel wt%. This may be quite evident and expected since hard nickel particles were mixed with base matrix and consequently contributed to effectively increase the hardness of the specimens (N1–N4). The utmost value was observed at 4 wt% nickel concentration, i.e. 740Hv. An improvement indicates the good bonding of nickel particles with modified Co–Cr–Mo alloys. A similar tendency was accounted by Savas and Alemdag [34] and Choudhary et al. [35] for the hardness of Al–40Zn–3Cu alloy and zinc–aluminium alloy with using nickel as a filler material, respectively. The authors investigated the influence of nickel (Ni) on the micro-structure and mechanical strength of the Zn–Al alloys.
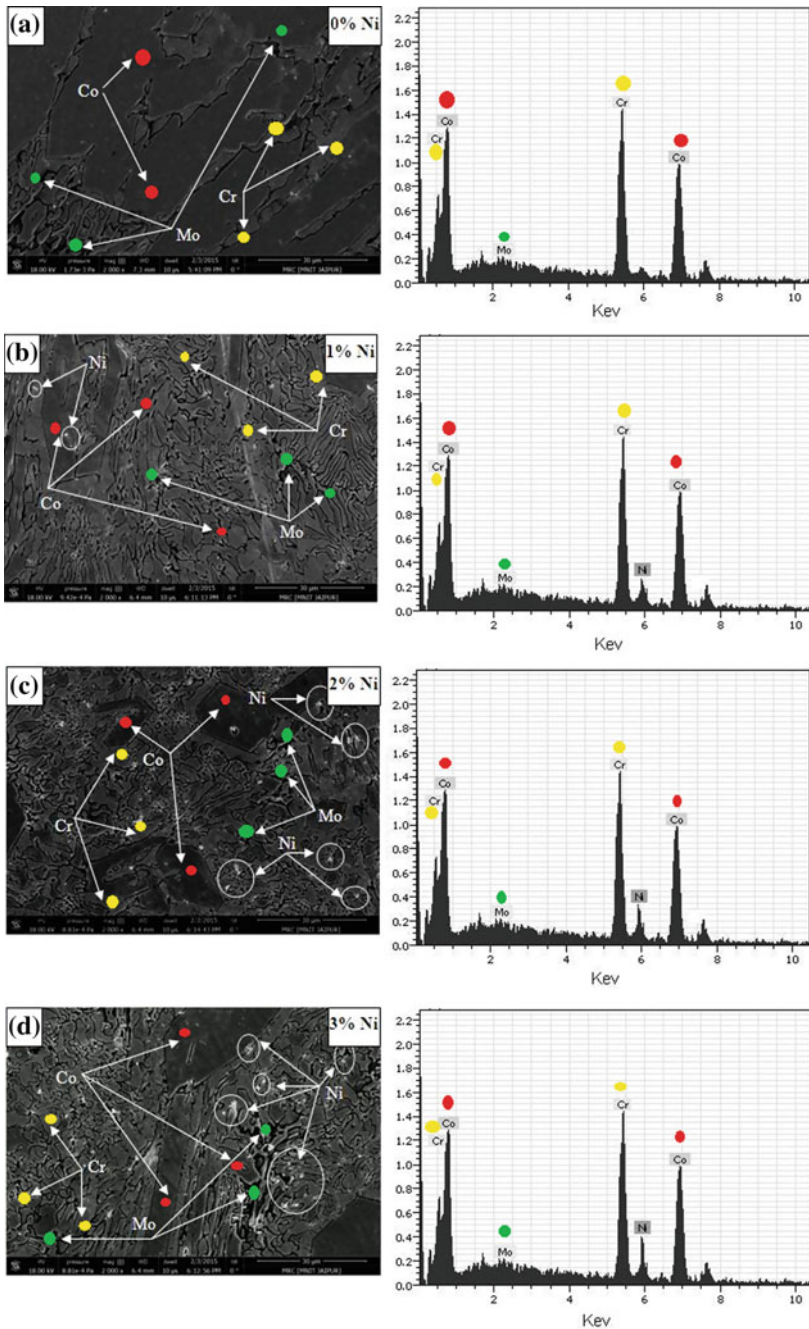
Fig. 5 FESEM micro-structure and corresponding EDX results of fabricated material with different nickel content: **a** N0, **b** N1, **c** N2, **d** N3 and **e** N4. Cobalt (Co), chromium (Cr), molybdenum (Mo) and nickel (Ni) are identified. Ni is shown just by the small white spots in the micro-structure
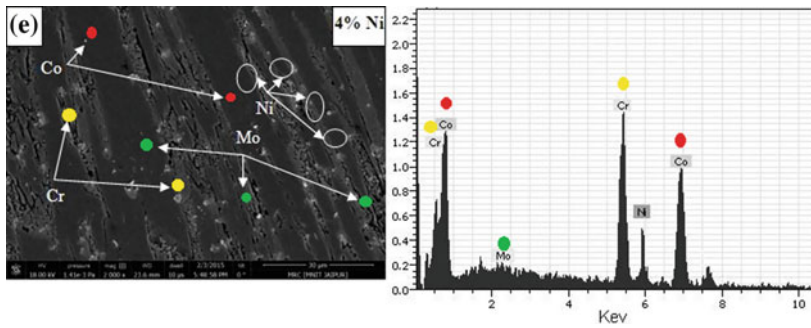
Fig. 5 (continued)

Table 5 Physico-mechanical properties of manufactured orthopaedic materials

Sample	Density (gm/cc)	Standard deviation	Hardness (HV)	Standard deviation
N0	8.7	0.01866	762	0.07891
N1	7.24	0.02175	590	0.48274
N2	7.8	0.01784	640	0.47539
N3	8.14	0.02156	690	0.18477
N4	8.58	0.01888	738	0.29489

3.4 Polarization Curves and Corrosion Behaviour of Manufactured Material

This analysis revealed that the accumulation of nickel has strong impact on their corrosion behaviour. Figure 6a represents the open-circuit potential (OCP or E_{OC}) for the Co–30Cr–4Mo alloys with the addition of different wt% of nickel worked as stationary electrodes when they were submerged in the NaCl solution at 37 °C and pH of 7.4. In this approach, the OCP of a metal varies as a function of time but stabilizes at a fixed value after a lengthy spell of immersion. If open-circuit potential is higher, then the material is characterized as better corrosion-resistant. Based on that and obtained results in Fig. 6a, after 1 h exposure, an approximately constant value of −0.29 V was attained when adding 4 wt% of nickel content in the alloying composition which was higher (see Fig. 6a) compared with those obtained for N1, N2 and N3.

Figure 6b and Table 6 show the anodic polarization curves of the fabricated Co–30Cr–4Mo alloy with distinct wt% of Ni and their corresponding corrosion parameters, respectively. As it can be seen in Table 6, the E_{corr} for 4 wt% of nickel-added alloy under NaCl solution was much more negative than those of 0–3 wt% Ni. Furthermore, the corrosion current of 4 wt% of nickel-added alloys was also much
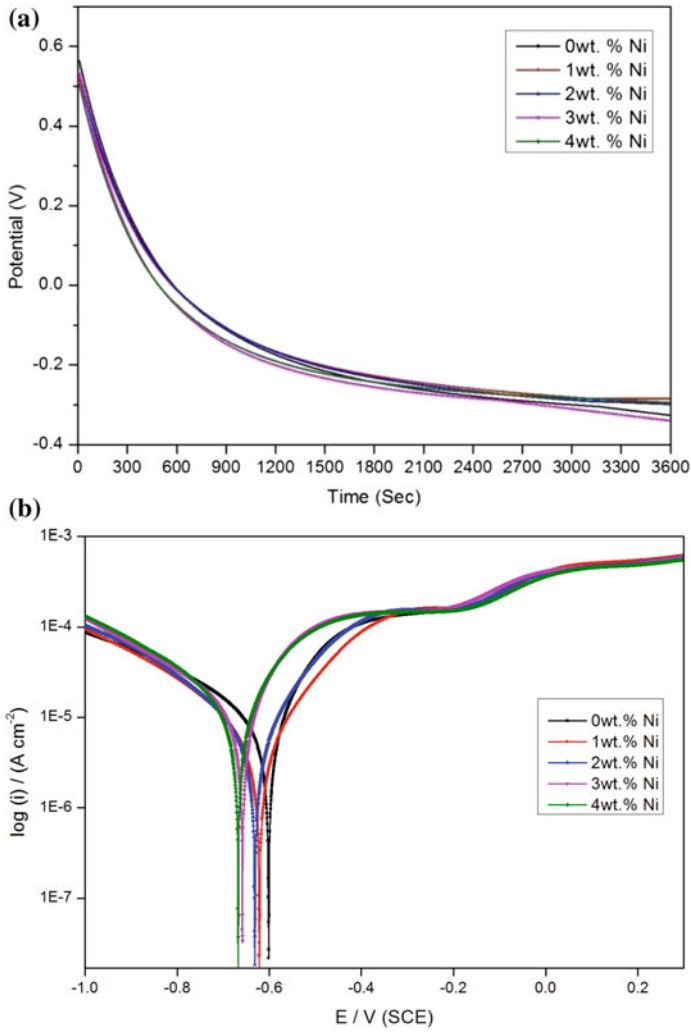
Fig. 6 **a** Open-circuit potential (OCP) curves and **b** Tafel polarization curves for different wt% of nickel

Table 6 Corrosion parameters for fabricated alloys at 37 °C with Tafel polarization method

Sample	I_{corr} (μA/cm^2)	E_{corr} (mV)	Corrosion rate (mm/year)
N0 (Co$_{30}$Cr$_4$Mo + 0 wt% Ni)	300	−689	0.499
N1 (Co$_{30}$Cr$_4$Mo + 1 wt% Ni)	184	−677	0.458
N2 (Co$_{30}$Cr$_4$Mo + 2 wt% Ni)	170	−658	0.432
N3 (Co$_{30}$Cr$_4$Mo + 3 wt% Ni)	164	−641	0.239
N4 (Co$_{30}$Cr$_4$Mo + 4 wt% Ni)	124	−626	0.221

larger as compared to among the samples. The corrosion current (I_{corr}) is directly proportional to the corrosion rate, thus minimal the value of corrosion current (I_{corr}) the better protection against corrosion. Therefore, the alloy N0 was identified as lower corrosion-resistant material. Similarly, the more positive or anodic the corrosion current, the higher the protection against corrosion. Hence, the alloy N4 was indicated to have higher corrosion resistance material. By definition, the corrosion of implants implies that a certain amount of ions is released from the implanted metal into the body. The liberated ions may be settled down in certain parts of the body causing biological reactions [36]. When the corrosion potentials and currents of prepared materials with different wt% nickel are compared, it can be seen that Co–30Cr–4Mo alloy with addition of 4 wt% of nickel in the material composition has a more positive corrosion potential and lower corrosion current as compared to the other weight percentage of nickel content alloys. Hence, it can be concluded that Co–30Cr–4Mo with the addition of 4 wt% of nickel is more stable against corrosion than others in biological media.

Figure 7 shows the surface micrographs for nickel-free and nickel-added Co–30Cr–4Mo alloys after immersion in saline (NaCl) solution at 37 °C with 7.4 pH. The morphology of specimen surface in Fig. 7a reveals that in the absence of nickel content, the surface was highly corroded (shown in black spot) with areas of localized corrosion. However, in the presence of the nickel content (see Fig. 7b) in the matrix material, the rate of corrosion was suppressed; this can be observed from the decrease of corroded areas (black spots). Again, with further increase in nickel content in the matrix material, i.e. 2 wt% Ni, the corroded area was further reduced; the small black spots in Fig. 7c. This is an expected response because the corrosion current, i.e. I_{corr} was low, i.e. ~170 µA/cm^2 (see Table 6), as compared to the other compositions. The lower is the corrosion current, the better its resistance to corrosion. By adding 3 wt% nickel to the alloy, the black spots (corroded surface) were further decreased (see Fig. 7d). However, addition of nickel in the alloy content, particularly 4 wt%, causes lower and smaller corroded areas (Fig. 7e). This is an expected response because the corrosion current, i.e. I_{corr} was low, i.e. ~124 µA/cm^2 (see Table 6) and less amount of ions was released and caused more resistance against corrosion.
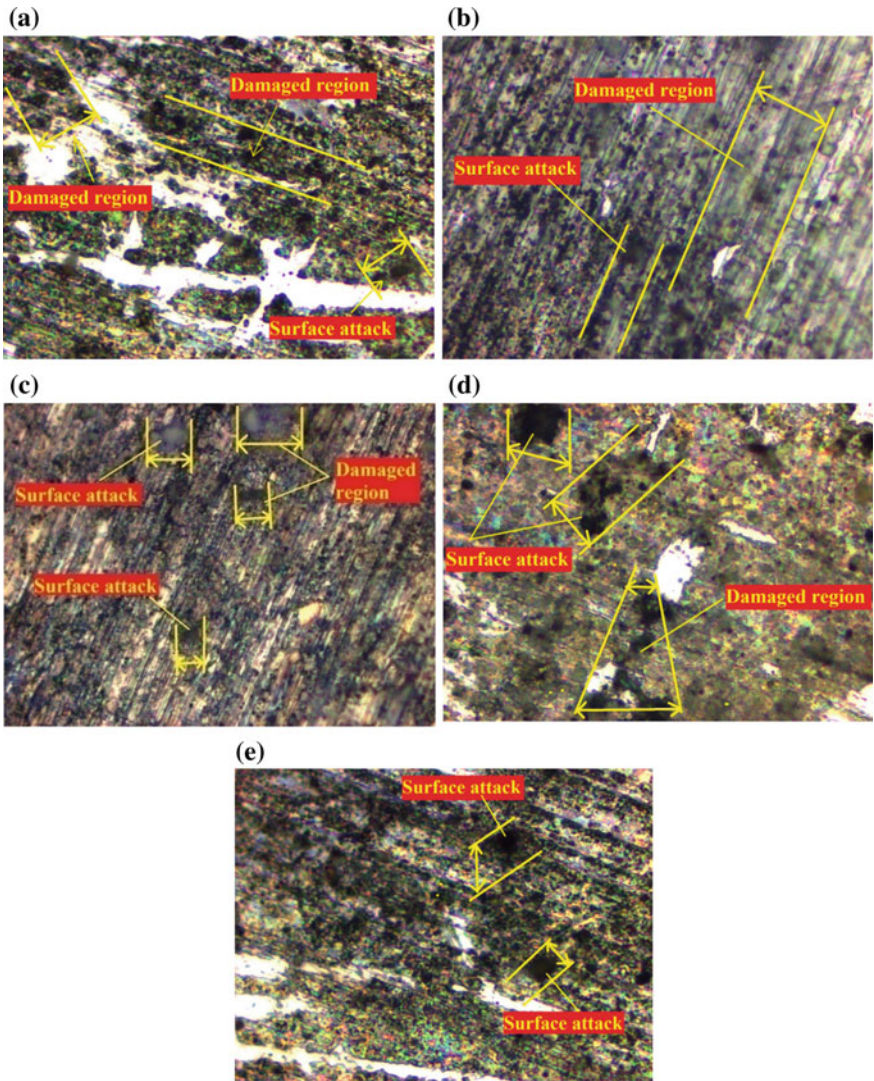
Fig. 7 Surface attack images of the tested specimens after 90 min immersion: **a** N0, **b** N1, **c** N2, **d** N3 and **e** N4 alloy

4   Conclusions

This is the first study on evaluation of the influence of nickel on mechanical strength and corrosion resistance of the recently developed Co–30Cr–4Mo alloy. It was found that the mechanical properties of the orthopaedic material enhanced after adding certain amount of nickel content in a beneficial way. From this study, it can be concluded that electrochemical data analysis and surface micrographs of manufactured orthopaedics materials containing with 4 wt% nickel exhibit superior corrosion resistance than others, hence recommended for hip implant materials. However, further research could assess the developed materials in other biological solutions such as serum and joint fluid.

References

1. Bhat SV (2005) Biomaterials, 2nd edn. Alpha Science International Ltd., Harrow
2. Alvarado J, Maldonado R, Marxuach J, Otero R (2003) Biomechanics of hip and knee prostheses. Applications of engineering mechanics in medicine. GED—University of Puerto Rico Mayaguez, pp 6–22
3. Bains PS, Mahajan R, Sidhu SS, Kaur S (2019) Experimental investigation of abrasive assisted hybrid EDM of Ti-6Al-4V. J Micromanuf. https://doi.org/10.1177/2516598419833498
4. Long M, Rack HJ (1998) Titanium alloys in total joint replacement-a materials science perspective. Biomater 19:1621–1639
5. Holzwarth U, Cotogno G (2012) Total hip arthroplasty. JRC Sci Policy rep. https://doi.org/10.2788/31286
6. Aherwar A, Singh A, Patnaik A (2016) Cobalt based alloy: a better choice biomaterial for hip implants. Trends Biomater Artif Organs 30(1):50–55
7. Cales B (2000) Zirconia as a sliding material-Histologic, laboratory, and clinical data. Clin Orthop Relat Res 379:94–112
8. Aherwar A, Singh A, Patnaik A (2016) Current and future biocompatibility aspects of biomaterials for hip prosthesis. J Bioeng 3(1):1–22
9. Aherwar A, Singh A, Patnaik A (2018) A study on mechanical behavior and wear performance of a metal-metal Co-30Cr biomedical alloy with different molybdenum addition and optimized using Taguchi experimental design. J Braz Soc Mech Sci Eng 40:213
10. Mirhosseini N, Crouse PL, Schmidth MJJ, Garrod D (2007) Laser surface micro-texturing of Ti–6Al–4V substrates for improved cell integration. Appl Surf Scie 253(19):7738–7743
11. Lewandowska-Szumiel M, Komender J, Chlopek J (1999) Interaction between carbon composites and bone after intrabone implantation. J Biomed Mater Res 48:289–296
12. Chang FK, Perez JL, Davidson JA (1990) Stiffness and strength tailoring of a hip prosthesis made of advanced composite materials. J Biomed Mater Res 24:873–899
13. Kauser F (2007) Corrosion of CoCrMo alloys for biomedical applications. University Birmingham, Metall Mater Sch Eng, pp 4–285
14. McMinn D, Daniel J (2006) History and modern concepts in surface replacement. Proc IMechE Part H: J Eng Med 220:239–251
15. Nomura N, Abe M, Kawamura A, Fujinuma S, Chiba A, Masahashi N, Hanada S (2006) Fabrication and mechanical properties of porous Co–Cr–Mo alloy compacts without Ni addition. Mater Trans 47(2):283–286
16. Bhui AS, Singh G, Sidhu SS, Bains PS (2018) Experimental investigation of optimal ED machining parameters for Ti-6Al-4V biomaterial. FU Mech Eng 16(3):337–345

17. Krasicka-Cydzik E, Oksiuta Z, Dabrowski J (2005) Corrosion testing of sintered samples made of the Co-Cr-Mo alloy for surgical applications. J Mater Sci Mater Med 16(3):197–202
18. Afolaranmi GA, Akbar M, Brewer J, Grant MH (2012) Distribution of metal released from cobalt–chromium alloy orthopaedic wear particles implanted into air pouches in mice. J Biomed Mater Res A 100(6):1529–1538
19. Moghaddam NS, Andani MT, Amerinatanzi A, Haberland C, Huff S, Miller M, Elahinia M, Dean D (2016) Metals for bone implants: safety, design, and efficacy. Biomanuf Rev 1:1
20. Bains PS, Grewal JS, Sidhu SS, Kaur S (2017) Wear between ring and traveler: a pin-on-disc mapping of various detonation gun sprayed coatings. Mater Today Proc 4(2):369–378
21. Rodrigues WC, Broilo LR, Schaeffer L, Knornschild G, Romel F, Espinoza M (2011) Powder metallurgical processing of Co-28% Cr-6% Mo for dental implants: Physical, mechanical and electrochemical properties. Powder Technol 206(3):233–238
22. Bahraminasab M, Hassan MR, Sahari BB (2010) Metallic biomaterials of knee and hip- a review. Trends Biomater Artif Organs 24(1):69–82
23. Hedberg Y, Wallinder IO (2014) Metal release and speciation of released chromium from a biomedical CoCrMo alloy into simulated physiologically relevant solutions. J Biomed Mater Res-Part B Appl Biomater 102(4):693–699
24. Panigrahi P, Liao Y, Mathew MT, Fischer A, Wimmer MA, Jacobs JJ, Marks LD (2014) Intergranular pitting corrosion of CoCrMo biomedical implant alloy. J Biomed Mater Res-Part B Appl Biomater 102(4):850–859
25. Kose N (2016) Biological response to orthopedic implants and biomaterials. In: Korkusuz FE (ed) Musculoskeletal res basic Sci. Springer, pp 3–14
26. Thakur RR, Ast MP, McGraw M, Bostrom MP, Rodriguez JA, Parks ML (2013) Severe persistent synovitis after cobalt–chromium total knee arthroplasty requiring revision. Orthop 36(4):e520–e524
27. Cadossi M, Mazzotti A, Baldini N, Gianini S, Savarino L (2016) New couplings, old problems: is there a role for ceramic-on-metal hip arthroplasty? J Biomed Mater Res Part B Appl Biomater 104(1):204–209
28. Ratner BD, Bankman I (2009) Biomedical engineering desk reference. Acad Press, Oxford
29. Montero-Ocampo C, Juarez R, Salinas-Rodriguez A (2007) Effect of FCC-HCP phase transformation produced by isothermal aging on the corrosion resistance of a Co-27Cr-5Mo-0.05C alloy. Metall Mater Trans A 33:2229–2235
30. Patel B, Inam F, Reece M, Edirisinghe M, Bonfield W, Huang J, Angadji A (2010) A novel route for processing cobalt–chromium–molybdenum orthopaedic alloys. J R Soc Interface 7:1641–1645
31. Rosenthal R, Cardoso BR, Bott IS, Paranhos RPR, Carvalho EA (2010) Phase characterization in as-cast F-75 Co–Cr–Mo–C alloy. J Mater Sci 45:4021–4028
32. ASTM F1537 (2000) Standard specification for wrought cobalt-28 chromium-6 molybdenum alloys for surgical implants. West Conshohocken, PA: ASTM Int
33. ASTM F75 (2014) Standard specification for cobalt-28 chromium-6 molybdenum alloy castings and casting alloy for surgical implants (UNS R30075). ASTM Int, Annual Book of Standards, West Conshohocken
34. Savas T, Alemdag Y (2010) Effect of nickel additions on the mechanical and sliding wear properties of Al–40Zn–3Cu alloy. Wear 268:565–570
35. Choudhury P, Das S, Datta BK (2002) Effect of Ni on the wear behaviour of a zinc-aluminium alloy. J Mater Sci 37:2103–2107
36. Basavarajappa S, Arun KV, Davim JP (2009) Effect of filler materials on dry sliding wear behavior of polymer matrix composites. J Min Mat Charact Eng 8(5):379–391